Identification of an inhibitory budding signal that blocks the release of HIV particles and exosome/microvesicle proteins

Xin Gan and Stephen J. Gould
Department of Biological Chemistry, Johns Hopkins University School of Medicine, Baltimore, MD 21205

ABSTRACT **Animal cells bud exosomes and microvesicles (EMVs) from endosome and plasma membranes. The combination of higher-order oligomerization and plasma membrane binding is a positive budding signal that targets diverse proteins into EMVs and retrovirus particles. Here we describe an inhibitory budding signal (IBS) from the human immunodeficiency virus (HIV) Gag protein. This IBS was identified in the spacer peptide 2 (SP2) domain of Gag, is activated by C-terminal exposure of SP2, and mediates the severe budding defect of p6-deficient and PTAP-deficient strains of HIV. This IBS also impairs the budding of CD63 and several other viral and nonviral EMV proteins. The IBS does not prevent cargo delivery to the plasma membrane, a major site of EMV and virus budding. However, the IBS does inhibit an interaction between EMV cargo proteins and VPS4B, a component of the endosomal sorting complexes required for transport (ESCRT) machinery. Taken together, these results demonstrate that inhibitory signals can block protein and virus budding, raise the possibility that the ESCRT machinery plays a role in EMV biogenesis, and shed new light on the role of the p6 domain and PTAP motif in the biogenesis of HIV particles.**

Monitoring Editor
Vivek Malhotra
Centre for Genomic Regulation

Received: Jul 23, 2010
Revised: Nov 23, 2010
Accepted: Jan 7, 2011

INTRODUCTION

Animal cells release small single-membrane vesicles (~50–250 nm) that have the same topology as the cell (Trams *et al.*, 1981; Pan and Johnstone, 1983; Gould *et al.*, 2003; Fang *et al.*, 2007; Schorey and Bhatnagar, 2008; Cocucci *et al.*, 2009; Simons and Raposo, 2009; Thery *et al.*, 2009). These vesicles mediate the release of specific proteins, lipids, mRNAs, and microRNAs; transmit signals to neighboring cells; and traffic molecules from the cytoplasm and membranes of one cell to the cytoplasm and membranes of others (Thery *et al.*, 2002; Valadi *et al.*, 2007; Skog *et al.*, 2008; Simons and Raposo, 2009). In addition, there is increasing evidence that these secreted vesicles play important roles in both normal physiological processes, such as immune signaling (Thery *et al.*, 2009) and development (Liegeois *et al.*, 2006; Kolotuev *et al.*, 2009), as well as in diseases such as cancer (Yu *et al.*, 2006; Yu *et al.*, 2009; Keller *et al.*, 2009), viral infections (Dukers *et al.*, 2000; Gould *et al.*, 2003; Fang *et al.*, 2007; Logozzi *et al.*, 2009; Nazarenko *et al.*, 2010), and amyloidopathies (Fevrier *et al.*, 2004; Leblanc *et al.*, 2006; Alais *et al.*, 2008).

It has been proposed that cells secrete small vesicles by two separate mechanisms, microvesicle biogenesis and exosome biogenesis (Cocucci *et al.*, 2009; Simons and Raposo, 2009). In this view, microvesicles bud from the plasma membrane, whereas exosomes are secreted by a two-step process in which vesicles 1) bud at endosomes to form multivesicular bodies (MVBs) and 2) are subsequently released after the fusion of MVBs with the plasma membrane. However, there is as yet no evidence that exosomes cannot bud from the plasma membrane, and there is significant evidence that plasma membranes can be a major site for budding of exosomal proteins, lipids, and their associated carbohydrates (Booth *et al.*, 2006; Fang *et al.*, 2007; Krishnamoorthy *et al.*, 2009; Marsh *et al.*, 2009). Furthermore, there is as yet no physical property or

This article was published online ahead of print in MBoC in Press (http://www.molbiolcell.org/cgi/doi/10.1091/mbc.E10-07-0625) on January 19, 2011.

Address correspondence to: Stephen Gould (sgould@jhmi.edu).

Abbreviations used: CA, capsid; DRM, detergent-resistant membrane; EIAV, equine infectious anemia virus; EMV, exosome/microvesicle; ESCRT, endosomal sorting complexes required for transport; FCS, fetal calf serum; GFP, green fluorescent protein; HIV, human immunodeficiency virus; HRP, horseradish peroxidase; HTLV-I, human T-lymphotropic virus; IBS, inhibitory budding signal; Ig, immunoglobulin; IP, immunoprecipitation; MA, matrix; mAb, monoclonal antibody; MVB, multivesicular body; NC, nucleocapsid; ORF, open reading frame; PBS, phosphate-buffered saline; RIPA, radio immunoprecipitation assay; RSV, Rous sarcoma virus; SIV, simian immunodeficiency virus; SP2, spacer peptide 2; TSG101, tumor suppressor gene 101; VPS, vacuolar protein sorting; WT, wild type.

molecular marker that can reliably differentiate microvesicles from exosomes once they are secreted (Simons and Raposo, 2009). These empirical and technical considerations make it difficult to distinguish exosomes from microvesicles, and we therefore refer to these vesicles by the collective acronym of EMV. The budding of human immunodeficiency virus (HIV) and other retroviruses shares many features with EMV biogenesis (Gould *et al.*, 2003), including the ability to bud from the surface of some cell types but via MVB-like structures in others (Morita and Sundquist, 2004; Freed and Martin, 2006; Marsh *et al.*, 2009).

One approach to understanding the biogenesis of secreted vesicles is to identify the *cis*-acting signals that target proteins to EMVs. We previously reported that the combination of plasma membrane binding and higher-order oligomerization is sufficient to target proteins to EMVs as well as their enrichment at sites of EMV budding (Fang *et al.*, 2007). In addition, we found that these same signals are sufficient to target proteins to HIV particles and are the primary budding signals in HIV Gag (Fang *et al.*, 2007), lending further support to the EMV model of retrovirus budding (Gould *et al.*, 2003). Although these observations advanced our understanding of protein and virus budding, they also raised a number of questions. For example, it is currently unclear how higher-order oligomerization and plasma membrane binding generate a biochemical signal. Also, there is no information on the cellular factors that recognize this signal, deliver cargo proteins to sites of budding, or catalyze EMV budding. This last aspect of the process is particularly perplexing, for there is a wealth of evidence that the endosomal sorting complexes required for transport (ESCRT) machinery can catalyze topologically identical budding events in vitro and is required for topologically similar events in vivo (e.g., MVB biogenesis, cytokinesis, and retrovirus budding [Saksena *et al.*, 2007; Hurley, 2008; Hanson *et al.*, 2009; Wollert *et al.*, 2009]). Nevertheless, the empirical evidence is that ESCRT dysfunction does not impair EMV biogenesis (Fang *et al.*, 2007; Trajkovic *et al.*, 2008). As for the factors that do promote EMV biogenesis, several have been identified, including Rab11 (Savina *et al.*, 2002), Rab27 (Ostrowski *et al.*, 2010), Rab35 (Hsu *et al.*, 2010), citron kinase (Loomis *et al.*, 2006), p53 (Yu *et al.*, 2006, 2009), TSAP6 (Yu *et al.*, 2006, 2009), neutral sphingomyelinase, and ceramide (Trajkovic *et al.*, 2008). However, it is still unclear how these factors combine to promote vesicle secretion.

Although the budding of HIV has attracted a great deal of attention, there is still no clear consensus about the regions of HIV Gag that are sufficient for its vesicular release. On one hand, there is strong evidence that higher-order oligomerization and plasma membrane binding are the primary budding signals in HIV Gag and that these lie within the matrix (MA), capsid (CA), and nucleocapsid (NC) domains of Gag, and not its C-terminal p6 domain (Demirov *et al.*, 2002; Fang *et al.*, 2007). On the other hand, there is strong evidence that the p6 domain might play a critical role in budding, as deletion of just the p6 domain can cause a severe defect in HIV budding from certain cell lines, including 293T cells (Gottlinger *et al.*, 1991; Demirov *et al.*, 2002). Here we sought to resolve these paradoxical results by identifying the *cis*-acting regions of HIV Gag that control its budding from 293T cells.

RESULTS

C-terminal exposure of spacer peptide 2 blocks the budding of HIV Gag

The precise removal of the p6 domain from HIV Gag can cause a severe defect in HIV budding from 293T and certain other cell types (Gottlinger *et al.*, 1991; Demirov *et al.*, 2002). On the basis of these (and other) observations, it has been proposed that the p6 domain represents the positive budding signal in HIV and HIV Gag (Morita and Sundquist, 2004; Bieniasz, 2009). However, it has also been demonstrated that loss of p6 has little or no effect on the budding of HIV from human T-cells (Demirov *et al.*, 2002; Fang *et al.*, 2007), a result that argues against a primary role for the p6 domain in Gag and virus budding. As a first step toward resolving this paradox, we tested whether HIV Gag displayed a similar dependence on its p6 domain for budding from 293T cells. Specifically, we transfected 293T cells with plasmids designed to express wild-type (WT) HIV Gag or a p6-deficient form of HIV Gag, Gag(p49). We then incubated the cells for 2 d, collected cells and secreted vesicles (EMVs), separated the samples by SDS–PAGE, and processed them for immunoblot using antibodies specific for HIV Gag. Loss of the p6 domain caused an approximately sevenfold decrease in budding (Figure 1B), to 15 ± 3.0% (average ± 1 SD) of WT HIV Gag ($n = 3$; $p = 4.3 \times 10^{-4}$). Thus deletion of the p6 domain causes a severe defect in the budding of Gag from 293T cells.

The severe budding defect caused by loss of the p6 domain is thought to be caused by the concomitant loss of specific ESCRT-binding motifs that lie within the p6 domain and, in particular, to the loss of the PTAP motif that binds the ESCRT protein tumor suppressor gene 101 (TSG101) (Garrus *et al.*, 2001; Morita and Sundquist, 2004; Bieniasz, 2009). If this model is correct, elimination of the PTAP motif, by mutating it to the amino acids LIRL (Huang *et al.*, 1995), should also cause a severe defect in budding. However, when we compared the budding of Gag($p6^{PTAP\text{-}LIRL}$) to that of Gag(p49) and WT HIV Gag (Figure 1B), we found that Gag($p6^{PTAP\text{-}LIRL}$) budded just as well as WT HIV Gag (110 ± 26%; $n = 3$; $p = 0.56$). Thus the severe budding defect of p6-deficient HIV Gag was not caused by loss of the PTAP motif. As for whether the budding defect might be caused by loss of an Alix-binding motif, the Gag protein we worked with in these studies lacks the p6-localized Alix-binding site found in some other HIV strains (Strack *et al.*, 2003).

Given that the severe budding defect of Gag(p49) is not caused by loss of the sole ESCRT-binding site (PTAP) in p6, we considered the possibility that some other difference was responsible for the severe budding defect of p6-deficient Gag. One obvious difference is that Gag(p49) has a new C terminus composed of the spacer peptide 2 (SP2) domain (SP2 has the sequence FLGKIWPSHKGRPGNF-$_{COOH}$ and lies between the NC and p6 domains of the Gag translation product; Figure 1A). To determine whether C-terminal exposure of SP2 might contribute to the budding defect of Gag(p49), we examined the effect of masking its C terminus. Specifically, we appended epitope tags to the C terminus of Gag(p49) and followed the budding of the resulting proteins (Figure 1B). Gag(p49)-3xmyc and Gag(p49)-SF budded far better than Gag(p49) and no differently from WT HIV Gag (80 ± 15% and 109 ± 28%, respectively; $n = 3$; $p = 0.15$ and 0.61, respectively). The SF tag is a 61 amino acid–long tag carrying four copies of the Strep tag and two copies of the Flag tag.

To further explore the idea that C-terminal exposure of SP2 might inhibit Gag budding, we followed the budding of Gag-SP2, a full-length HIV Gag protein containing an additional copy of the SP2 peptide appended to its C terminus. 293T cells were transfected with plasmids designed to express either WT HIV Gag or Gag-SP2 and incubated for 2 d, and then cell and EMV lysates were collected. Immunoblot analysis of these samples using anti-Gag antibodies revealed a severe budding defect for Gag-SP2 (Figure 1C), only 4.2 ± 3% relative to the WT control ($n = 4$; $p = 6.3 \times 10^{-6}$). This result demonstrates that C-terminal exposure of SP2 has a potent inhibitory effect on Gag budding. Additional experiments revealed

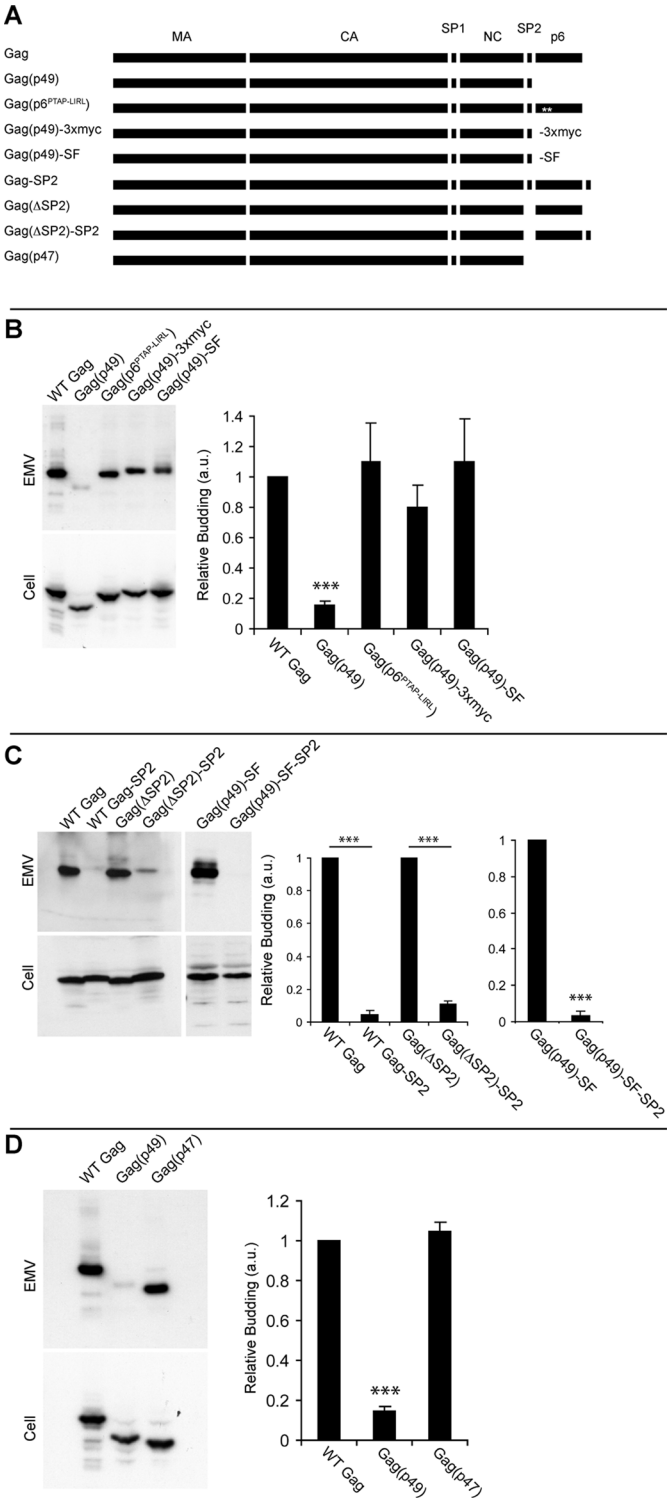

FIGURE 1: Identification of an inhibitory budding signal. (A) Line diagram of Gag proteins. (B–D) Immunoblots of EMV and cell lysates from 293T cells expressing WT and mutant Gag proteins, probed with antibodies specific for HIV Gag. As with all experiments in this study, the cells were transfected with equal amounts of plasmid, and EMVs and cells were loaded at the same ratio. Furthermore, bar graphs of relative budding (in arbitrary units) display the average (solid bar) and SD (error brackets) from at least three trials, relative to WT control, where *** denotes a p value < 0.0005, ** denotes a p value < 0.005, and * denotes a p value < 0.05. (B) Immunoblot of EMV and cell lysates from 293T cells expressing WT HIV Gag, Gag(p49), Gag($p6^{PTAP-LIRL}$), Gag(p49)-3xmyc, and Gag(p49)-SF. The bar graph to the right displays the relative budding in arbitrary units. (C) Immunoblot of EMV and cell lysates from 293T cells expressing WT HIV Gag, Gag-SP2, Gag(ΔSP2), Gag(ΔSP2)-SP2, Gag(p49)-SF, and Gag(p49)-SF-SP2, with the bar graph to the right showing the relative budding from multiple trials. (D) Immunoblot of EMV and cell lysates from 293T cells expressing WT HIV Gag, Gag(p49), and Gag(p47). As above, the bar graph shows the relative budding efficiency of each protein, expressed as described above.

that the internal copy of SP2 in WT HIV Gag did not inhibit its budding and did not contribute significantly to the poor budding of Gag-SP2 (Figure 1C). The potent effect of exposing SP2 at the C terminus was also observed in the context of Gag(p49)-SF (Figure 1C), as Gag(p49)-SF-SP2 budded very poorly, only 1.7 ± 0.8% in comparison to Gag(p49)-SF ($n = 3$; $p = 2.3 \times 10^{-5}$).

These results support the hypothesis that the severe budding defect displayed by Gag(p49) is also caused by C-terminal exposure of SP2. If true, a Gag protein with a slightly larger deletion, one that removes the p6 domain and also the inhibitory elements within SP2, should bud from 293T cells nearly as well as WT HIV Gag. To test this prediction, we compared the budding of Gag(p49) to that of Gag(p47), which lacks all of p6 and also the C-terminal 12 amino acids of SP2 (Figure 1D). In each of three trials we observed that this shorter protein, Gag(p47), budded as well as WT HIV Gag (103 ± 7%; $p > 0.05$) and far better than Gag(p49) (14 ± 3% of WT; $n = 3$; $p < 0.0005$). These data demonstrate that the budding defect of p6-deficient HIV Gag was caused primarily by C-terminal exposure of SP2 and not by loss of any positive budding information that may reside within the p6 domain.

C-terminal exposure of SP2 activates a *cis*-acting inhibitory budding signal

The inhibitory effect of C-terminal SP2 exposure could be restricted to just HIV Gag. Alternatively, it could reflect the existence of an inhibitory budding signal (IBS) that can impair the budding of heterologous proteins. To distinguish between these possibilities, we appended the C-terminal 12 amino acids of SP2 ($IWPSHKGRPGNF_{COOH}$, which we refer to as SP2*) to the C terminus of several other budding-competent proteins and assayed their budding from 293T cells. Gag proteins from retroviruses typically bud well from animal cells, and SF-tagged versions of the equine infectious anemia virus (EIAV), Rous sarcoma virus (RSV), and human T-lymphotropic virus 1 (HTLV-1) Gag proteins all budded at high levels from 293T cells (Figure 2A). Moreover, we found that addition of SP2* to the C terminus of these proteins impaired their budding from 293T cells (Figure 2A), to 24 ± 2% in the case of EIAV Gag-SF-SP2* ($n = 3$; $p = 0.0002$), 5.2 ± 7% in the case of RSV Gag-SF-SP2* ($n = 3$; $p = 0.002$), and 5.7 ± 5% in the case of HTLV-1 Gag-SF-SP2* ($n = 3$; $p = 8 \times 10^{-6}$). Given that the HIV, EIAV, RSV, and HTLV-I Gag proteins lack significant amino acid sequence similarity and share only a single, short motif (ΩXXXEXXXXXΦXRO) within their CA domains (Benit *et al.*, 1997), these results indicate that C-terminal exposure of SP2* activates an IBS that can block the budding of heterologous proteins.

To test whether the activity of the IBS extended to nonviral EMV proteins, we created plasmids designed to express SF-tagged forms of CD63 and CD63-SP2*, transfected these into 293T cells, and assayed EMV and cell lysates for the relative budding of each protein. CD63 is an integral membrane protein that is secreted in EMVs by numerous cell types and is the most commonly used marker of EMVs (Simons and Raposo, 2009). CD63-SF budded well from 293T cells (Figure 2B), demonstrating that this C-terminally tagged form of human CD63 is an EMV cargo protein. The budding of

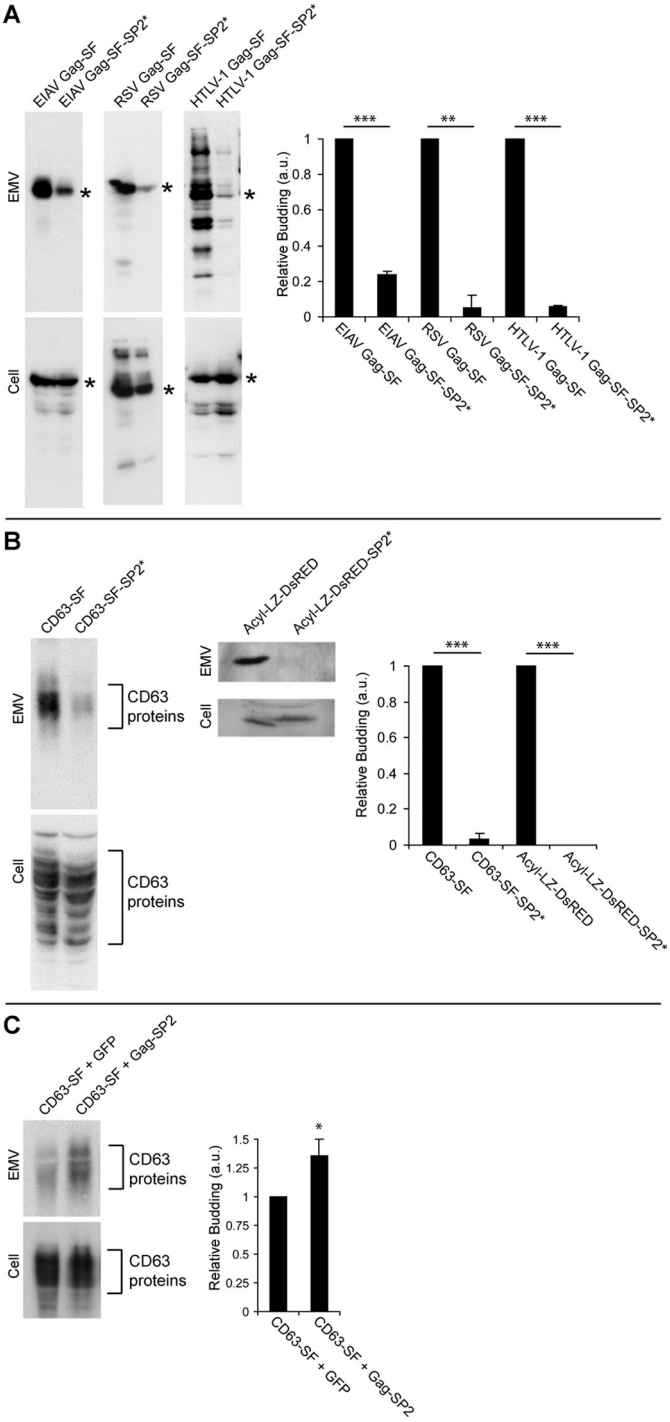

FIGURE 2: The IBS inhibits the budding of heterologous proteins. (A) Immunoblots of EMV and cell lysates from 293T cells expressing (left blots) EIAV Gag-SF and EIAV Gag-SF-SP2*, (center blots) RSV Gag-SF and RSV Gag-SF-SP2*, and (right blots) HTLV-1 Gag-SF and HTLV-1 Gag-SF-SP2*, probed with anti-Flag antibodies specific for the SF tag. Asterisks denote the primary translation product, and the bar graph displays the average and SD of their relative budding. (B) Immunoblots of EMV and cell lysates from 293T cells expressing (left blots) CD63-SF and CD63-SF-SP2*, and (right blots) Acyl-LZ-DsRED and Acyl-LZ-DsRED-SP2*, probed with antibodies specific for the SF tag or DsRED, respectively. CD63 is heavily and heterogeneously glycosylated, giving rise to proteins with varying M_r that are highlighted by brackets. The bar graph to the right displays the relative budding data from a minimum of three trials, as described above. (C) Anti-Flag immunoblots of EMV and cell lysates from 293T cells expressing 1) CD63-SF and GFP or 2) CD63-SF and Gag-SP2. CD63 is once again highlighted with brackets, and the data from multiple trials are presented in the bar graph to the right.

CD63-SF-SP2* was substantially less than CD63-SF (3.0 ± 3%; n = 3; p = 0.0004), supporting the hypothesis that C-terminal exposure of SP2* activates an IBS. We also examined the effect of the IBS on Acyl-LZ-DsRED (Fang *et al.*, 2007). Acyl-LZ-DsRED budded well from 293T cells whereas Acyl-LZ-DsRED-SP2* displayed no detectable budding from these cells (Figure 2B).

We next tested whether the IBS impaired the budding of all EMV cargoes from the cell or whether its effect was limited to the protein to which it was attached. To do this we cotransfected 293T cells with plasmids designed to express 1) the EMV marker CD63-SF and 2) either green fluorescent protein (GFP) or Gag-SP2. After incubating the cells for 2 d, we collected cell and EMV lysates and processed them for immunoblot using antibodies specific for the SF tag. The budding of CD63-SF was no less in cells expressing Gag-SP2 than in cells expressing GFP (Figure 2C), indicating that expression of an IBS-containing cargo does not impair EMV budding in general. In fact, expression of Gag-SP2 led to a slight increase in the budding of CD63-SF, to 140 ± 14% (n = 3; p = 0.047).

Mutational analysis of the IBS

To better understand the structural basis for IBS function, we performed a series of mutational studies, using Gag-SP2 as the test protein. Deletion of just the C-terminal amino acid, F16, resulted in a Gag-SP2 protein that budded quite well from 293T cells, and loss of additional residues from the SP2 C terminus had similar effects (Figure 3, A and B). Removing the N-terminal 2 or 4 amino acids of SP2 had little if any effect on IBS activity, while deletion of the N-terminal 7 amino acids impaired IBS activity, and larger deletions seemed to eliminate IBS function altogether (Figure 3, A and B). These observations are consistent with 1) the ability of the C-terminal 12 amino acids of SP2 (SP2*, amino acids 5–16 of SP2) to block the budding of viral and nonviral EMV cargoes, and 2) the observation that removing SP2* is what allowed Gag(p47) to bud much better than Gag(p49) and nearly as well as WT HIV Gag (see Figure 1D).

On the basis of these results, it appeared that the IBS was located within the 12 amino acids from Ile-5 to Phe-16. To identify the amino acids within this region that are critical to IBS function, we replaced each of them with alanine, again in the context of the Gag-SP2 protein (Figure 3C). Consistent with our previous observations, Gag-SP2 budded poorly, 4.2 ± 3% (n = 4; p < 0.0005) relative to full-length HIV Gag. Similar results were observed for Gag-SP2 variants in which alanine had been substituted for Pro-7 (5.8 ± 3%), Ser-8 (9.9 ± 4%), His-9 (8.2 ± 3%), Lys-10 (4.8 ± 3%), Gly-11 (6.6 ± 2%), or Gly-14 (4.2 ± 2%), indicating that these amino acids do not play essential roles in IBS function (numbers are from four trials, and in all cases there was no significant difference from the budding of Gag-SP2 (p > 0.05). In contrast, substituting alanine for several other residues effectively eliminated IBS activity, seen here by the high levels of budding detected for the Ile-5A (190 ± 16%, relative to full-length HIV Gag), Trp-6A (210 ± 8%), Arg-12A (190 ± 22%), Pro-13A (200 ± 22%), Asn-15A (240 ± 25%), and Phe-16A (130 ± 13%) variants of Gag-SP2 (n = 4; p < 0.005). These mutants also budded slightly more than WT HIV Gag (p < 0.05).

Although the single alanine substitutions identified several critical residues within the IBS, these particular alanine substitution

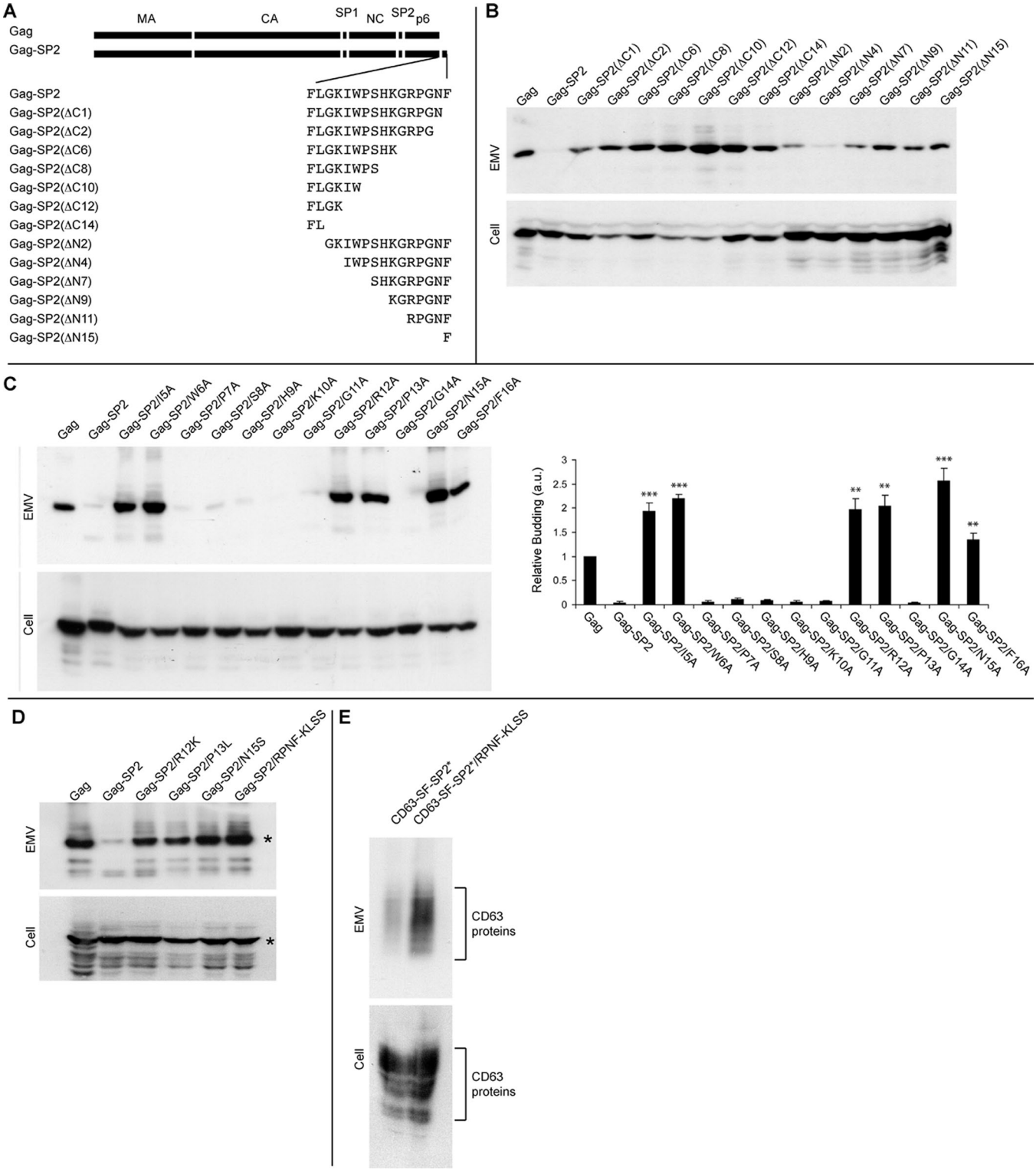

FIGURE 3: Mutational analysis of the IBS. (A, B) Deletion analysis of the IBS. (A) Line diagram displaying the organization of Gag, Gag-SP2, and the amino acid sequences of the SP2 deletion mutants generated in the Gag-SP2 protein. (B) Anti-Gag immunoblots of EMV and cell lysates from 293T cells expressing WT HIV Gag, Gag-SP2, and the ΔN and ΔC mutations of the C-terminal SP2 peptide. (C) Alanine scanning mutagenesis of the IBS. Anti-Gag immunoblots were performed on EMV and cell lysates from 293T cells expressing WT HIV Gag, Gag-SP2, and alanine substitution mutants of the 12 amino acids that lie within the functional domain of SP2. The bar graph to the right shows the relative budding of each protein ascertained from three independent trials. (D) Anti-Gag immunoblots of EMV and cell lysates from 293T cells expressing WT HIV Gag, Gag-SP2, and four variants of Gag-SP2 that carried virus-compatible mutations of critical residues of the IBS. (E) Anti-Flag immunoblots of EMV and cell lysates from 293T cells expressing CD63-SF-SP2* and a variant of CD63-SF-SP2* that has the four–amino acid substitution mutation in the SP2 peptide, RPNF to KLSS.

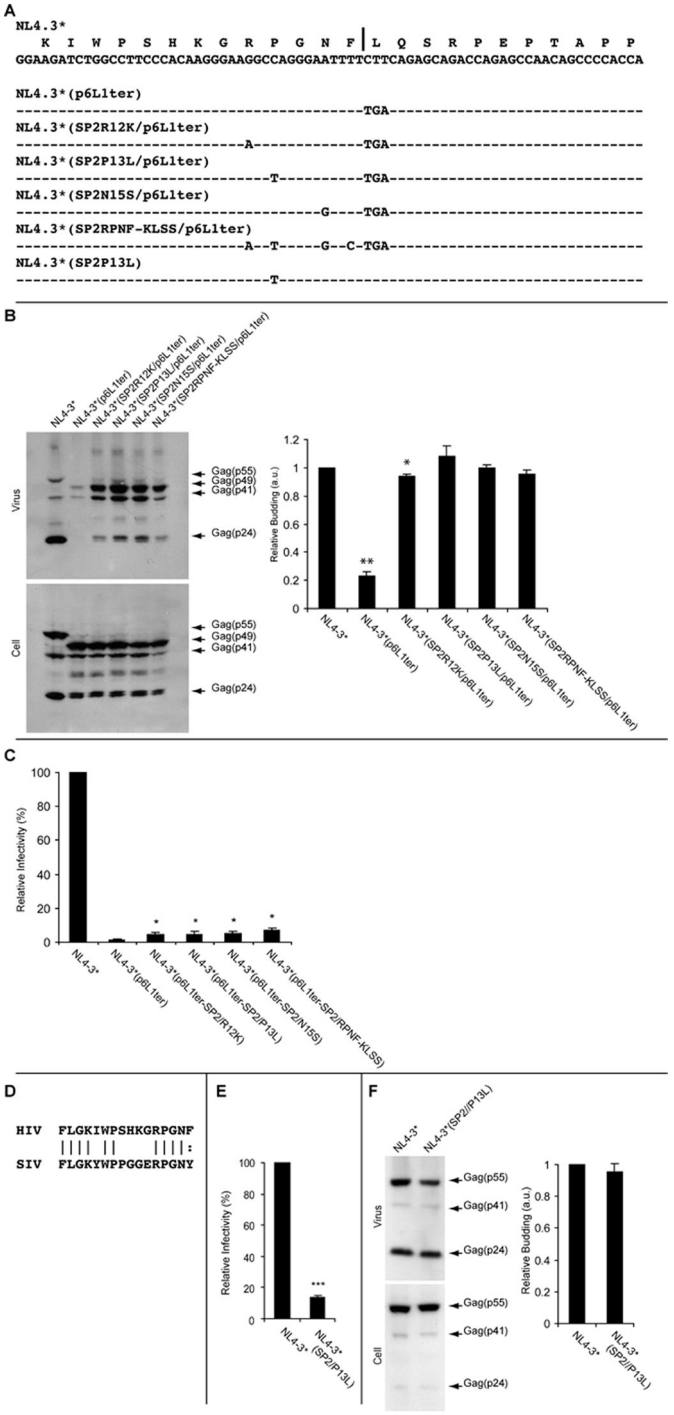

FIGURE 4: Inactivation of the IBS suppresses the budding defect of p6-deficient HIV and reduces HIV infectivity. (A) Sequences of HIV and relevant HIV mutants. Top line is the deduced amino acid sequence of the Gag ORF in the vicinity of the SP2/p6 junction, denoted by the vertical line between GNF and LQS. The next line shows the positions of the DNA sequence changes in the corresponding mutant proviruses. (B) Anti-Gag immunoblot of virus and cell lysates from 293T cells expressing control HIV (NL4.3*), p6-deficient HIV (NL4-3*[$p6^{L1ter}$]), and variants of p6-deficient HIV that have inactivating mutations in the IBS (NL4-3*[$p6^{L1ter}$/$SP2^{R12K}$], NL4-3*[$p6^{L1ter}$/$SP2^{P13L}$], NL4-3*[$p6^{L1ter}$/$SP2^{N15S}$], and NL4-3*[$p6^{L1ter}$/$SP2^{RPNF-KLSS}$]). The p55 and p49 Gag proteins are the primary translation products of the control and p6-deficient proviruses, respectively. The p41 products are generated by Gag cleavage at either of the PR sites that lie between CA and NC. The p24/25 CA products are generated by additional cleavage of p41 between MA and CA. Note that most of the Gag protein in viruses produced by WT HIV is fully cleaved (p24) whereas most of the Gag protein detected in the viruses produced by p6-deficient HIV is either uncleaved (p49) or cleaved at one or two of the sites that lie between CA and NC (p41). The relative budding efficiencies of each virus are presented in the bar graph to the right, and in all cases the p value was calculated relative to WT control. (C) Relative infectivity of the same control and mutant viruses as in (B). The p values for the infectivity of the doubly mutant viruses are in relation to the infectivity of NL4-3*($p6^{L1ter}$). (D) BLAST alignment of the HIV SP2 domain with the SIV Gag protein shows the conservation of many IBS residues. (E) Relative infectivity of NL4.3* and NL4.3*($SP2^{P13L}$), presented as the average ± 1 SD, with *** denoting a p value < 0.0005. Anti-Gag immunoblot of virus and cell lysates from 293T cells expressing control and mutant viruses. (F) Anti-Gag immunoblot of virus and cell lysates of 293T cells expressing NL4.3* and NL4.3*($SP2^{P13L}$), with the averages ± 1 SD presented graphically at the right.

mutations cannot be introduced into an HIV proviral clone without also changing the amino acid sequence of the Gag-Pol polyprotein (the ribosomal frameshift in the translation of the Gag open reading frame [ORF] to generate the Gag-Pol protein occurs just upstream of the SP2 coding region [Freed and Martin, 2006]). We therefore examined the relative budding of four additional substitution mutations in SP2, three single amino acid substitutions ($SP2^{R12K}$, $SP2^{P13L}$, and $SP2^{N15S}$) and a four–amino acid substitution ($SP2^{RPNF-KLSS}$). Each of these mutations impaired IBS function in the context of the Gag-SP2 protein (Figure 3D).

We also tested whether one of these mutations could inactivate the IBS in the context of a nonviral EMV cargo. For this we compared the budding of CD63-SF-SP2* to that of CD63-SF-SP2*$^{RPNF-KLSS}$. The budding of CD63-SF-SP2*$^{RPNF-KLSS}$ was higher than that of CD63-SF-SP2* (Figure 3E), consistent with the hypothesis that these residues play an important role in IBS activity.

IBS inactivation suppresses the budding defect of p6-deficient HIV

The preceding observations demonstrated that the severe budding defect of p6-deficient HIV is effectively phenocopied by p6-deficient HIV Gag protein and that this budding defect is caused primarily by C-terminal exposure of SP2 and the concomitant activation of an IBS. However, our studies were carried out on a Gag protein from a different strain (type C) than that used in most studies on HIV budding (type B). Moreover, they were carried out on Gag and not virus. To determine whether our findings were relevant to a type B HIV strain, we tested whether the IBS was responsible for the severe budding defect of a p6-deficient from of NL4.3, a commonly used type B clone. NL4.3* is our designation for NL4-3-ΔE-GFP, a variant of NL4.3 designed for measuring HIV infectivity (Zhang *et al.*, 2004) and the parental clone we used for all experiments. To eliminate p6 expression, we used the $p6^{L1ter}$ mutation, which terminates the HIV Gag ORF at the first codon (Leu) of p6 and causes a severe budding defect in 293T cells (Huang *et al.*, 1995; Demirov *et al.*, 2002; Fang *et al.*, 2007).

To explore the contribution of the IBS to the budding defect of p6-deficient HIV, we introduced IBS-inactivating mutations into NL4.3*($p6^{L1ter}$), transfected control and mutant proviruses into 293T cells, collected cells and viruses, and processed cell and virus lysates for immunoblot using anti-Gag antibodies. As expected, NL4.3* budded well from 293T cells, whereas the budding of NL4.3*($p6^{L1ter}$) was significantly reduced, only 23 ± 3% of control (n = 3; $p = 5.5 \times 10^{-4}$) (Figure 4B). In contrast, forms of NL4.3*($p6^{L1ter}$)

that carried inactivating mutations in the IBS budded at nearly WT levels, 94 ± 2% for NL4.3*(SP2^{R12K}/p6^{L1ter}), 110 ± 7% for NL4.3*(SP2^{P13L}/p6^{L1ter}), 100 ± 2% for NL4.3*(SP2^{N15S}/p6^{L1ter}), and 96 ± 3% for NL4.3*(SP2$^{RPNF\text{-}KLSS}$/p6^{L1ter}) (n = 3; p = 0.024, 0.18, 0.96, and 0.12, respectively). These data demonstrate that inactivation of the IBS suppresses the budding defect of p6-deficient HIV. As such, these observations provide strong evidence that the budding defect of p6-deficient virus is caused primarily by the C-terminal exposure of SP2 and the concomitant activation of the IBS, and not by loss of any positive budding information that might reside within the p6 domain.

The IBS contributes to HIV infectivity

We also assessed the relative infectivity of these viruses. For this we took advantage of the fact that NL4.3* allows one to measure the infectivity of mutant HIV viruses by direct visualization of transfected and infected cells (NL4.3* encodes a form of GFP that is localized to the endoplasmic reticulum [Zhang *et al.*, 2004]). In brief, we 1) cotransfected HIV proviruses into 293T cells together with a plasmid designed to express VSV-G, a fusogenic ENV protein (Zhang *et al.*, 2004); 2) incubated the cells for 2 d; 3) collected virus samples; 4) used them to infect CD4$^+$ T-cells; and 5) scored the relative infectivity of each provirus by counting the number of NL4.3*-expressing (GFP-positive) T-cells, normalized to the number of NL4.3*-expressing 293T cells in the first phase of the assay (Zhang *et al.*, 2004). These experiments revealed that the p6^{L1ter} mutation reduced HIV infectivity ~50-fold (Figure 4C), to 1.4 ± 0.2% of WT HIV (n = 4; p < 0.0005). In contrast, we observed a three- to fivefold increase in the infectivity of p6-deficient HIV when the IBS was also inactivated, to 7.6 ± 0.9% for NL4-3*(p6^{L1ter}/SP2$^{RPNF\text{-}KLSS}$), 4.5 ± 0.6% for NL4-3*(p6^{L1ter}/SP2^{R12K}), 5.1 ± 0.8% for NL4-3*(p6^{L1ter}/SP2^{P13L}), and 5.2 ± 1% for NL4-3*(p6^{L1ter}/SP2^{N15S}).

On the basis of these observations, it appears that IBS inactivation fully suppresses the budding defect of p6-deficient HIV but only partially suppresses its infectivity defect. This is not surprising when one considers that 1) the HIV accessory protein Vpr plays critical postentry roles in the HIV life cycle (Freed and Martin, 2006), and 2) loss of p6 eliminates the Vpr-binding site that HIV uses to recruit Vpr into nascent virions (Paxton *et al.*, 1993; Freed and Martin, 2006). Moreover, the fact that the IBS has potent biological activity and is conserved between simian immunodeficiency virus (SIV) and HIV (Figure 4D) raises the possibility that the IBS might itself contribute to HIV infectivity. To test this hypothesis, we introduced the SP2^{P13L} mutation into NL4.3* and determined its effect on HIV infectivity. The P13L mutation reduced HIV infectivity approximately sevenfold (Figure 4D), to 15 ± 2% of control (n = 3; p < 0.0005). This effect was not caused by a drop in HIV budding (Figure 4E) as this virus budded at the same level as WT control (96 ± 5%; n = 4; p = 0.27). These data demonstrate that the IBS plays a positive role in the HIV life cycle.

The budding defect of PTAP-deficient HIV requires Gag-Pol and the IBS

We next attempted to understand why PTAP-deficient HIV Gag buds at nearly WT levels (see Figure 1, A and B) whereas PTAP-deficient virus has a budding defect as severe as p6-deficient HIV, seen here by the poor budding of both NL4.3*(p6$^{PTAP\text{-}LIRL}$) and NL4.3*(p6^{L1ter}) (Figure 5, A and B). Intriguingly, cells expressing PTAP-deficient HIV generated significantly higher levels of Gag(p49) than the control virus. This raised the possibility that loss of the PTAP motif results in the activation of the IBS, via the aberrant, PR-mediated cleavage of Gag at the SP2/p6 junction.

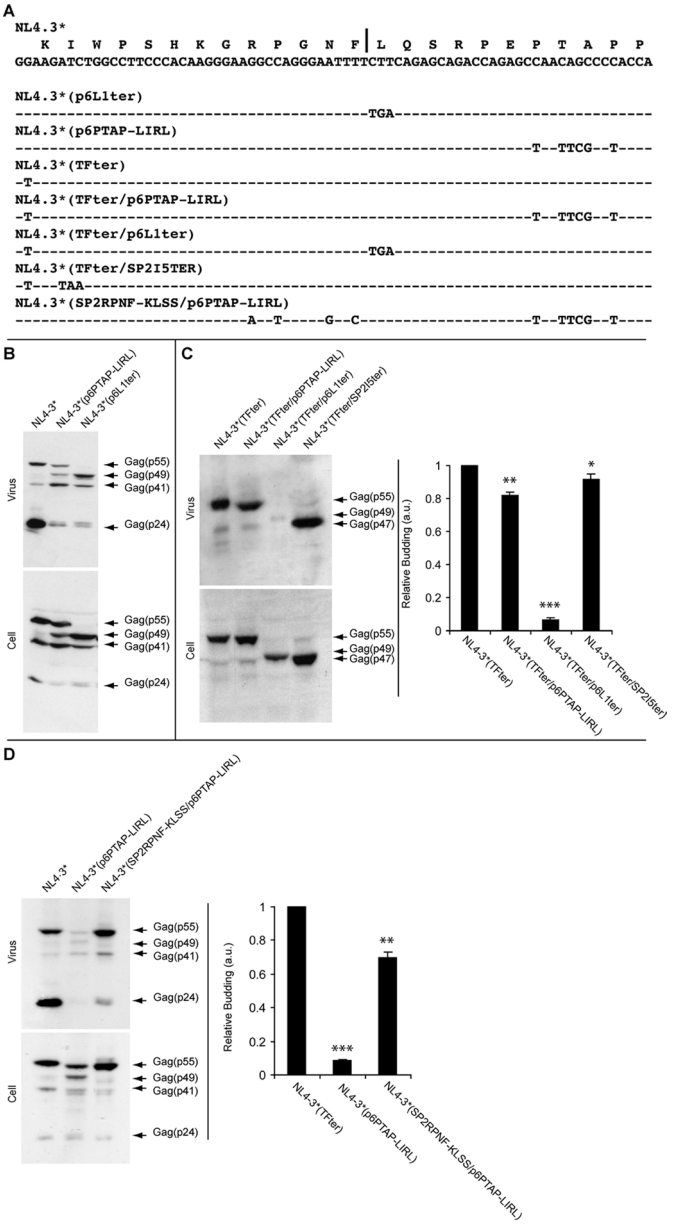

FIGURE 5: Gag-Pol and the IBS are required for the budding defect of PTAP-deficient HIV. (A) Sequences of HIV and relevant HIV mutants. Top line is the deduced amino acid sequence of the Gag ORF in the vicinity of the SP2/p6 junction, denoted by the vertical line between GNF and LQS. The next line shows the positions of the DNA sequence changes in the corresponding mutant proviruses. (B) Anti-Gag immunoblot of virus and cell lysates from 293T cells expressing control HIV (NL4.3*), p6-deficient HIV (NL4-3*[p6^{L1ter}]), and PTAP-deficient HIV (NL4-3*[p6$^{PTAP\text{-}LIRL}$]). (C) Anti-Gag immunoblot of virus and cell lysates from 293T cells expressing NL4.3*(TF^{ter}), NL4.3*(TF^{ter}/p6$^{PTAP\text{-}LIRL}$), NL4.3*(TF^{ter}/p6^{L1ter}), and NL4.3*(TF^{ter}/SP2^{I5ter}), with the averages and SD plotted to the right. (D) Anti-Gag immunoblot of virus and cell lysates from 293T cells expressing NL4.3*, NL4.3*(TF^{ter}/p6$^{PTAP\text{-}LIRL}$), and NL4.3*(SP2$^{RPNF\text{-}KLSS}$/p6$^{PTAP\text{-}LIRL}$), with the averages and SD plotted to the right.

If this hypothesis is correct, it should be possible to suppress the budding defect of PTAP-deficient HIV by eliminating expression of the Gag-Pol polyprotein (the viral protease, PR, is generated only via expression of Gag-Pol [Freed and Martin, 2006]). To test this prediction, we created a form of HIV, NL4.3*(TF^{ter}), that is unable to

express the Gag-Pol polyprotein due to a nonsense mutation in the transframe region of the Gag-Pol ORF (the TF^{ter} mutation blocks Gag-Pol translation but does not alter the predicted translation product of the Gag ORF [Figure 5A]). Following transfection of 293T cells with the corresponding proviruses, we found that the TF^{ter} mutation suppressed most of the budding defect caused by loss of the PTAP motif: NL4.3*(TF^{ter}/$p6^{PTAP\text{-}LIRL}$) budded from cells at 83 ± 2% (n = 4; p = 0.0054) of that seen for NL4.3*(TF^{ter}). In contrast, the TF^{ter} mutation did not suppress the budding defect of p6-deficient HIV (Figure 5C), as NL4.3*(TF^{ter}/$p6^{L1ter}$) budded at only ~7% the level of NL4.3*(TF^{ter}) (6.9 ± 1%; n = 4; $p = 9.9 \times 10^{-6}$). The budding defect of NL4.3*(TF^{ter}/$p6^{L1ter}$) could, however, be suppressed by elimination of SP2, shown here by the nearly normal budding of NL4.3*(TF^{ter}/$SP2^{I5ter}$) (92 ± 3% relative to control; n = 4; p = 0.012). This virus has a stop codon in place of Ile-5 of the SP2 domain, expresses neither the IBS nor the p6 domain, and budded ~13-fold more than NL4.3*(TF^{ter}/$p6^{L1ter}$).

If the budding defect of PTAP-deficient HIV involves the PR-mediated activation of the IBS, it should also be suppressed by inactivating mutations in the IBS. To test this prediction, we compared the budding of NL4.3*, NL4.3*($p6^{PTAP\text{-}LIRL}$), and NL4.3*($SP2^{RPNF\text{-}KLSS}$/$p6^{PTAP\text{-}LIRL}$). Following the transfection of 293T cells with the corresponding viruses, we found that NL4.3*($p6^{PTAP\text{-}LIRL}$) budded at 8.7 ± 0.4% of control virus (n = 3; $p = 5.3 \times 10^{-6}$) and that inactivation of the IBS largely suppressed this budding defect (Figure 5D), elevating it eightfold to 70 ± 3% of control (n = 3; p = 0.001).

The IBS does not block membrane binding

In an effort to understand how the IBS might function, we first examined its effect on the membrane-binding activity of HIV Gag. 293T cells were transfected with plasmids designed to express HIV Gag or HIV Gag-SP2, incubated for 2 d, and lysed in hypotonic buffer to generate membrane fragments. The lysates were adjusted at a high concentration of sucrose (73%) and split into several tubes, and then one portion was fractionated by sucrose density flotation gradient centrifugation. Under these conditions, free proteins remain at the bottom of the gradient whereas membrane-associated proteins float to upper fractions due to the low density of the membranes to which they are attached. When the resulting fractions were assayed for the presence of Gag proteins by immunoblot, we found that both Gag and Gag-SP2 floated out of the initial, high-density fraction into the lower density fractions, as expected for membrane-associated proteins (Figure 6A). The only difference in the behavior of Gag-SP2 was that it was more highly enriched in the membrane-associated fractions (140 ± 18%; n = 3; p = 0.050).

To test whether the flotation of these proteins was truly due to their association with membranes, we preincubated an aliquot of each lysate with 0.25% Triton X-100 for 20 min at 37°C, a treatment that is known to solubilize biological membranes. These samples were also subjected to sucrose density gradient centrifugation, and the resulting fractions were analyzed by immunoblot using anti-Gag antibodies. Following this treatment, neither protein floated out of the initial high-density fractions (Figure 6B). In contrast to treatment with warm Triton X-100, treatment with cold Triton X-100 fails to fully solubilize membrane domains that are enriched in cholesterol and sphingolipids (Edidin, 2003; Lingwood *et al.*, 2009), and HIV Gag is enriched in these detergent-resistant membrane (DRMs) fractions (Nguyen and Hildreth, 2000; Ono and Freed, 2001). To determine whether the IBS might impair this aspect of Gag activity, we added cold Triton X-100 to yet another portion of the lysates and then subjected them also to sucrose density gradient centrifugation. Gag and Gag-SP2 were both enriched in DRMs (Figure 6C), though

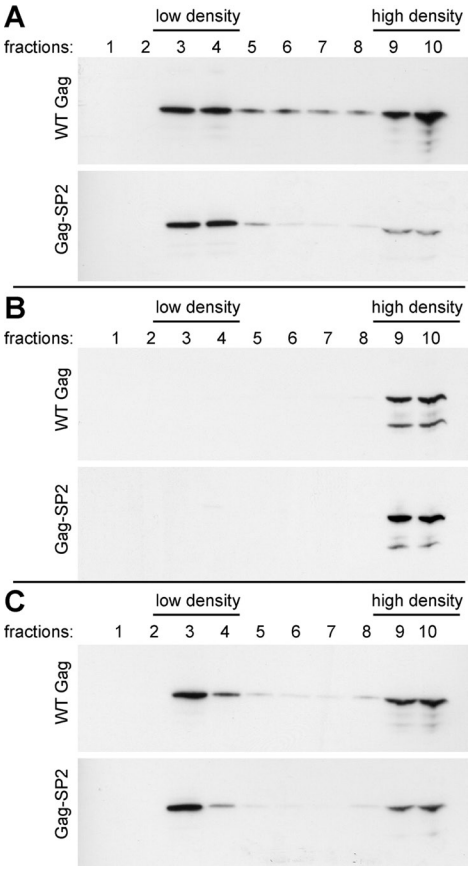

FIGURE 6: The IBS does not impair membrane binding. (A–C) Anti-Gag immunoblots of fractions from sucrose density flotation gradients that were carried out on (A) cell lysates from 293T cells expressing (top) HIV Gag and (bottom) Gag-SP2, (B) cell lysates from 293T cells expressing (top) HIV Gag and (bottom) Gag-SP2 that had been preincubated with 0.25% Triton X-100 for 20 min at 37°C, and (C) cell lysates from 293T cells expressing (top) HIV Gag and (bottom) Gag-SP2 that had been preincubated with 0.25% Triton X-100 for 20 min at 4°C. Fractions were collected from the top of the gradient, with fraction 1 having the lowest density and fraction 10 having the highest density.

Gag-SP2 showed a slightly greater enrichment in DRM fractions (140 ± 3%; n = 3; p = 0.002) than WT Gag.

The IBS does not prevent plasma membrane localization

We next tested whether the IBS might act by preventing its trafficking to the plasma membrane. Immunofluorescence microscopy revealed that WT HIV Gag was distributed throughout the cell (Figure 7, A–D), consistent with prior reports on the steady-state distribution of this protein (Freed, 1998; Freed and Martin, 2006; Morita and Sundquist, 2004). In contrast, Gag-SP2 was highly enriched at the plasma membrane and in many cells was concentrated at large patches of the plasma membrane (Figure 7, E–H). Thus the IBS did not prevent the trafficking of Gag to the plasma membrane. This conclusion is also supported by the trafficking of Gag(p49), which was also enriched at the plasma membrane (Figure 7, I and J). In contrast, Gag(p47) displayed an intracellular distribution that more closely resembled that of WT HIV Gag, with no apparent enrichment at the plasma membrane (Figure 7, K and L). Perhaps the simplest interpretation of these data is that the inability of IBS-activated proteins to bud from cells merely causes

them to accumulate at the prior step in their journey, the plasma membrane.

We also tested the effect of the IBS on the subcellular localization of CD63-SF. This protein buds well from 293T cells (see Figure 2) and localizes to the plasma membrane, and addition of the IBS did not prevent its plasma membrane localization (Figure 7, M–P). These images are representative of >90% of expressing cells, and each protein was examined in 100 or more expressing cells. Additional images of expressing cells are available as supplemental material (Supplemental Figures S1–S6).

The plasma membrane enrichment of Gag-SP2 should also be apparent in transmission electron micrographs, as the highly oligomeric Gag complex forms an electron-dense lamina under membranes to which it is attached (Freed and Martin, 2006). 293T cells expressing WT HIV Gag were surrounded by numerous vesicles containing the electron-dense lamina (Figure 7, Q and R). Cells expressing Gag-SP2 differed in that they failed to secrete Gag-containing vesicles and instead contained a Gag-SP2 lamina underlying large patches of the plasma membrane (Figure 7, S–U). Although we occasionally detected cell profiles in which the Gag-SP2 lamina extended from the plasma membrane (Figure 7V), these were "headless" extensions that bore no resemblance to the budding intermediates that accumulate in cells expressing the classic late-domain mutant Gag(p6$^{PTAP\text{-}LIRL}$) (Figure 7, W and X). Given that the accumulation of trapped budding intermediates is the defining characteristic of a "late" budding defect, the IBS appears to block Gag budding at an earlier stage in the budding process.

The IBS does not prevent Gag-Gag oligomerization

Protein budding, including the budding of HIV and HIV Gag, is driven by a combination of plasma membrane targeting and higher-order oligomerization (Fang *et al.*, 2007). Given that Gag-Gag

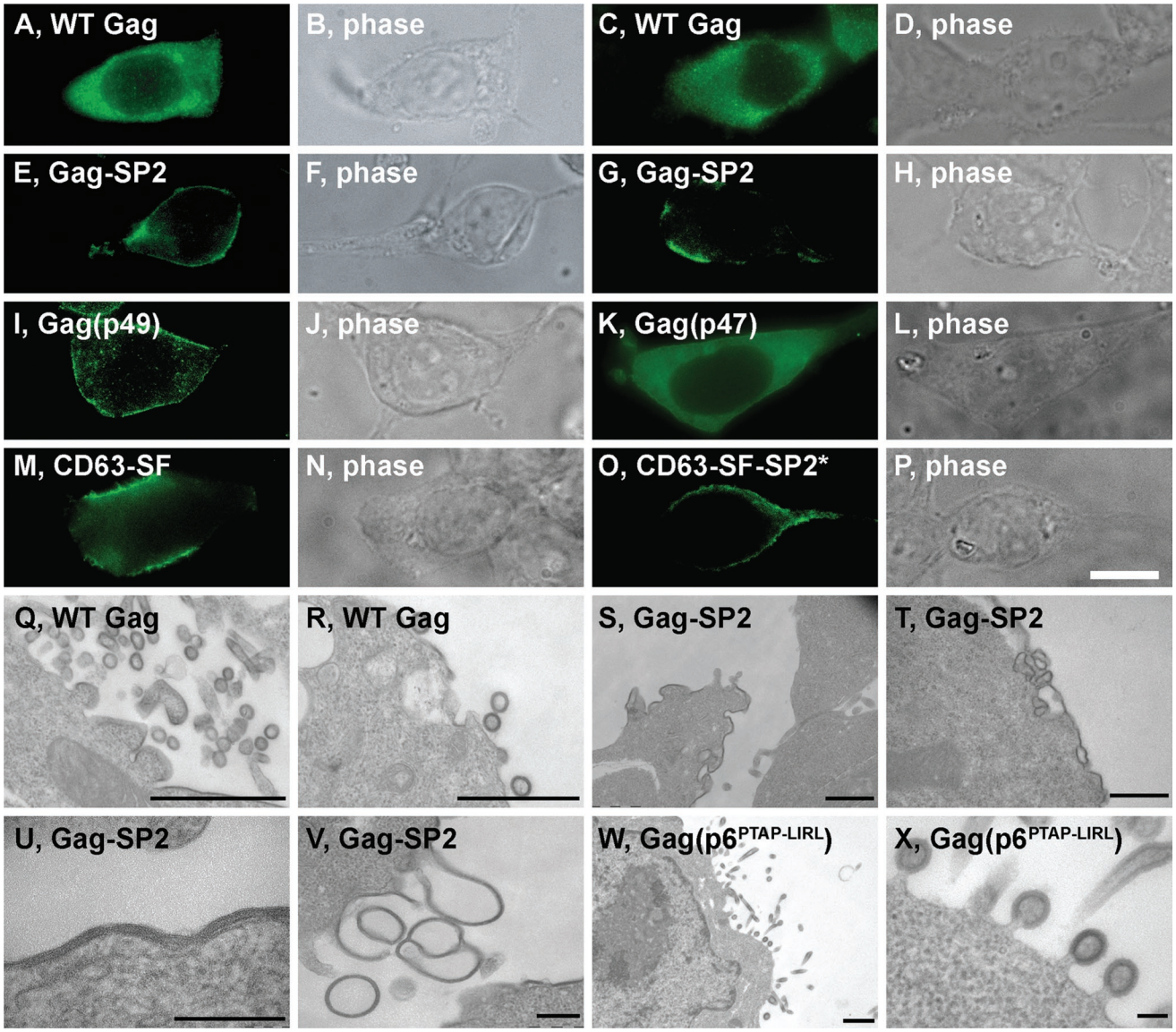

FIGURE 7: The IBS does not block plasma membrane localization. (A–P) Fluorescence and phase microscopy of 293T cells expressing (A–D) WT HIV Gag, (E–H) HIV Gag-SP2, (I, J) HIV Gag(p49), (K, L) HIV Gag(p47), (M, N) CD63-SF, and (O, P) CD63-SF-SP2*. Bar, 10 μm. The images shown here are representative of what was seen in greater than 90% of expressing cells, with at least 100 expressing cells examined for each protein tested. (Q–X) Transmission electron microscopy of 293T cells expressing (Q, R) WT HIV Gag, (S–V) HIV Gag-SP2, or (W, X) HIV Gag(p6$^{PTAP\text{-}LIRL}$). Bar, 1 μm for Q–T, V, and W; bar, 100 nm for U and X.

oligomerization is required for the formation of an electron-dense lamina such as that seen in 293T cells expressing Gag-SP2, it is unlikely that the IBS impairs cargo budding by preventing its oligomerization. Furthermore, it is unclear how such a short peptide (12 amino acids) could impair the budding of so many structurally unrelated cargoes (retroviral Gag proteins, CD63, Acyl-LZ-DsRED). Nevertheless, we assessed the effect of the IBS on Gag-Gag coimmunoprecipitation. As a prelude to such experiments, we tested whether Gag and Gag-SP2 proteins carrying an N-terminal AcylSF tag (specifying N-terminal acylation and containing multiple Strep and Flag tags) retained the relative budding activities of untagged Gag and Gag-SP2. They did (Figure 8A). Next, we cotransfected 293T cells with plasmids designed to express 1) Gag-3xmyc and 2) either AcylSF-Gag or AcylSF-Gag-SP2. Two days later we lysed the cells in detergent buffer, immunoprecipitated Gag-3xmyc, and probed the resulting immunoprecipitates for the presence of AcylSF-Gag or AcylSF-Gag-SP2, respectively. These experiments revealed that the IBS did not reduce Gag-Gag coimmunoprecipitation (Figure 8B).

HIV Gag forms oligomeric complexes with upward of 1000 Gag subunits and a size of 50 MDa, well above the resolution of size exclusion chromatography. Nevertheless, Gag assembly in vivo proceeds from small oligomers, and thus it is formally possible that gel filtration chromatography might nevertheless expose some differences in the oligomerization profile of Gag and Gag-SP2. Toward this end we transfected 293T cells with plasmids designed to express either WT Gag or Gag-SP2, lysed the cells in radio immunoprecipitation assay (RIPA) buffer, fractionated the lysates on a Sephacryl-500 gel filtration resin (size exclusion limit of ~500 kDa), and assayed each fraction by immunoblot using antibodies specific for HIV Gag and β-tubulin (Figure 8C). The elution profiles of Gag and Gag-SP2 were very similar, but there appeared to be a slightly higher proportion of Gag-SP2 in the late void volume fractions, 5 and 6. As with the enhanced plasma membrane localization of Gag-SP2, this difference might be a relatively simple consequence of the severe budding defect of Gag-SP2 because the higher-order oligomerization of WT Gag leads to its release from the cell.

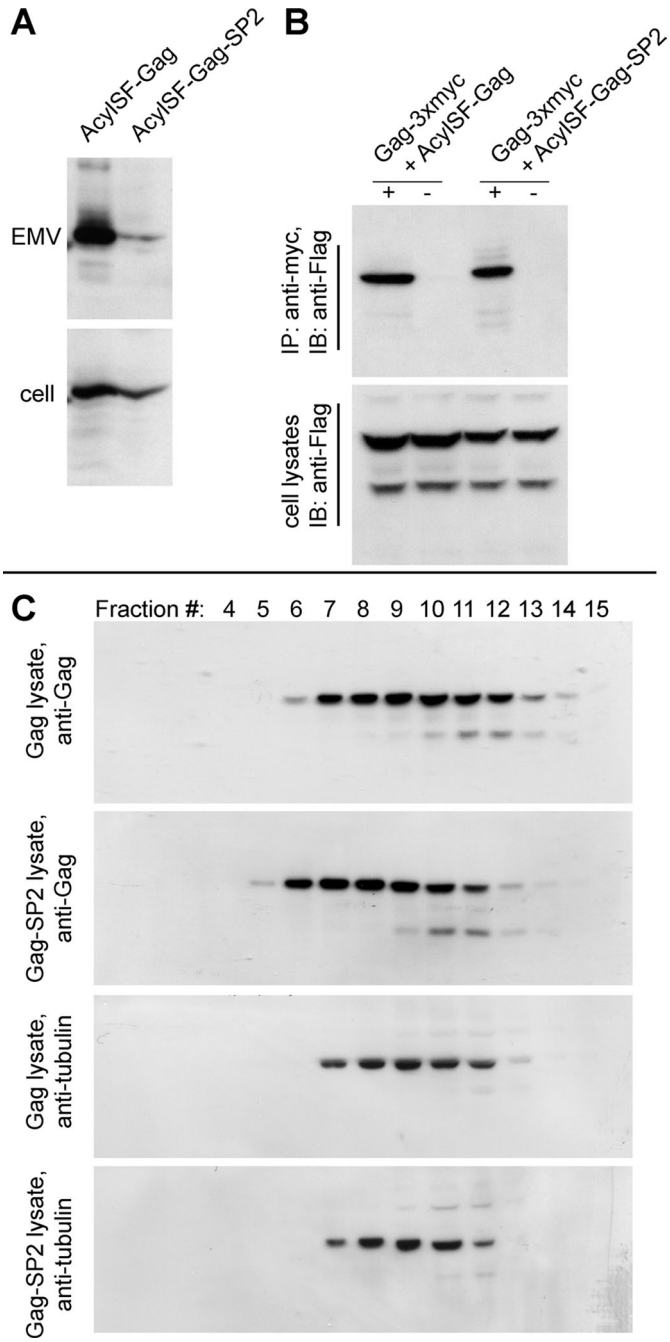

FIGURE 8: The IBS does not impair Gag-Gag oligomerization. (A) Anti-Flag immunoblot of EMV and cell lysates from 293T cells expressing AcylSF-Gag and AcylSF-Gag-SP2. (B) Top, anti-Flag immunoblot of anti-myc IPs generated from 293T cells expressing Gag-3xmyc and either AcylSF-Gag or AcylSF-Gag-SP2. Bottom, anti-Flag immunoblot of the input, 27% of what was used in the IP reaction. The + lanes were IPs with anti-GFP antibodies; the – lanes were IPs with nonimmune IgG. (C) Gel filtration eluates of 293T cell lysates expressing either HIV Gag or Gag-SP2 were processed for immunoblot using antibodies specific for (top two panels) HIV Gag or (bottom two panels) β-tubulin.

IBS activation impairs an EMV cargo–VPS4 interaction

The ESCRT proteins comprise the only machinery that is known to catalyze outward vesicle budding (Saksena *et al.*, 2007; Hurley, 2008; Bieniasz, 2009; Wollert *et al.*, 2009). This role has been demonstrated in vitro and is consistent with the observation that ESCRT dysfunction inhibits MVB biogenesis, cytokinesis, and HIV budding. Although the inhibition of ESCRT function does not prevent EMV budding (Fang *et al.*, 2007; Trajkovic *et al.*, 2008), a role for the ESCRT machinery in EMV biogenesis cannot be excluded. We therefore explored the possibility that EMV cargoes might interact with the ESCRT machinery. Specifically, we explored the possibility that EMV cargoes interacted with vacuolar protein sorting 4 (VPS4), an ESCRT-associated ATPase that binds and disassembles complexes of ESCRT proteins and their cargoes (Hurley, 2008; Wollert *et al.*, 2009). 293T cells were cotransfected with plasmids designed to express GFP-VPS4B together with various EMV cargoes, incubated for 2 d, and then lysed. GFP-VPS4B and associated proteins were subjected to immunoprecipitation (IP) using anti-GFP or control antibodies, and the resulting IPs were examined by SDS–PAGE and immunoblot using antibodies specific for the EMV cargoes. These experiments revealed that there is a specific interaction between GFP-VPS4B with CD63-SF (Figure 9A). Furthermore, we found that the presence of the IBS at the C terminus of CD63-SF significantly impaired this interaction. We also detected a specific interaction between GFP-VPS4B and CD81-SF, and this too was significantly reduced by the presence of the IBS (Figure 9B). Similar results were observed for Gag(p47), which buds from cells and showed a significant interaction with GFP-VPS4B. In contrast, the 12 amino acid–longer Gag(p49) protein, which exposes the IBS at its C terminus and buds poorly from cells, showed little if any specific interaction

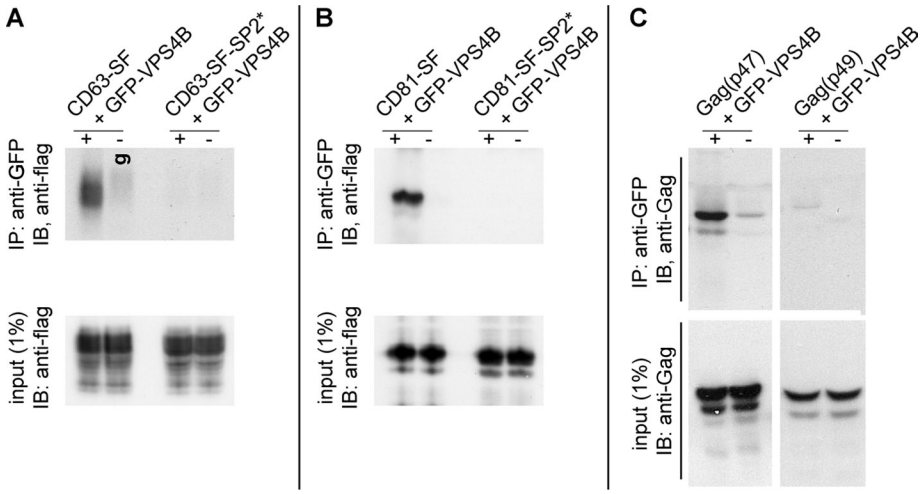

FIGURE 9: The IBS impairs an interaction between EMV cargoes and VPS4B. (A–C) Immunoblots of (top) coimmunoprecipitations and (bottom) cell lysates generated from 293T cells coexpressing GFP-VPS4B and (A) CD63-SF or CD63-SF-SP2*, (B) CD81-SF or CD81-SF-SP2*, or (C) Gag(p47) or Gag(p49). The + lanes were IPs with anti-GFP antibodies, the – lanes were IPs with nonimmune IgG. Immunoblots were with 1% of IP input.

with GFP-VPS4B (Figure 9C). These data represent the first evidence that there is an interaction between the ESCRT machinery and budding-competent proteins. Furthermore, they demonstrate that the IBS attenuates this interaction. These data do not, however, demonstrate a direct physical interaction between VPS4B and EMV cargoes or that the IBS impairs protein budding by impairing this cargo–ESCRT interaction.

DISCUSSION

The observation that higher-order oligomerization and plasma membrane binding can target diverse proteins to secreted vesicles (Fang *et al.*, 2007) solved part of the question of how proteins are targeted to exosomes, microvesicles, and virus-like particles. The data presented here extend our understanding of EMV biogenesis by demonstrating that IBSs can also have a significant impact on the biogenesis of EMV proteins and the budding of HIV. In addition, our findings shed new light on the molecular basis for the severe budding defect caused by loss of the HIV p6 domain or by mutation of the ESCRT-binding PTAP motif.

How does the IBS block cargo protein budding?

The identification of the IBS raises the question of how it functions. One possibility is that the IBS might interfere with the *cis*-acting determinants of protein trafficking to EMVs, which are the combination of plasma membrane binding and higher-order oligomerization. The IBS did not inhibit the ability of proteins to interact with membranes or their trafficking to the plasma membrane. In fact, activation of the IBS in HIV Gag appeared to increase its plasma membrane localization. As for whether the IBS impairs cargo oligomerization, it is difficult to imagine how a short (12-residue) peptide like the IBS could block the oligomerization of such different proteins as CD63, Acyl-LZ-DsRED, and the Gag proteins from HIV, EIAV, RSV, and HTLV-1. Furthermore, the IBS did not prevent Gag oligomers from attaining their electron-dense appearance in transmission EM experiments, did not prevent Gag-Gag co-IP, and did not reduce its apparent oligomerization as assessed by gel filtration chromatography. On the other hand, it is not clear how higher-order oligomerization converts a protein from a non-EMV cargo into an efficient EMV cargo, and thus it is possible that the IBS could yet act by affecting its EMV targeting information.

An alternative possibility is that the IBS might act by perturbing an interaction between EMV cargoes and whatever cellular machinery binds EMV cargoes and mediates their budding from the cell. Although such factors have yet to be identified, the ESCRT machinery has been implicated in other modes of outward vesicle budding (e.g., MVB biogenesis, HIV budding, and cytokinesis). We therefore tested whether EMV cargoes might interact, directly or indirectly, with a key ESCRT-associated factor, the AAA ATPase VPS4B. The classic exosomal markers CD63 and CD81 both copurified with VPS4B, the first evidence for any involvement of the ESCRT machinery with EMV biogenesis. Furthermore, the IBS inhibited these cargo–VPS4B interactions. These results raise the possibility that the ESCRT machinery plays a positive role in EMV biogenesis and that the IBS inhibits cargo protein budding by impairing this interaction. Consistent with this hypothesis, we found that VPS4B interacted with HIV Gag(p47) but showed less interaction with Gag(p49). However, additional studies are still needed to elucidate the significance of cargo–ESCRT interactions, the mechanistic basis for IBS function, and the reason why the IBS impairs the co-IP between VPS4B and EMV proteins.

Implications for HIV budding

There is no empirical discrepancy between our results and those of previous studies vis-à-vis the budding of p6-deficient HIV or PTAP-deficient HIV (Gottlinger *et al.*, 1991; Demirov *et al.*, 2002; Morita and Sundquist, 2004). However, our observations demonstrating the existence of the IBS, its potent inhibitory effects on protein and virus budding, and the ability of IBS-inactivating mutations to suppress the budding defects of p6-deficient and PTAP-deficient HIV alter the interpretation of these classic observations. Specifically, our data undermine the hypothesis that the severe defect in budding seen for the PTAP-deficient and p6-deficient virus is because the virus has lost critical "budding signals." In its place, our data suggest a new paradigm in which the budding defects of these particular mutant viruses are caused by activation of the IBS, either directly in the case of p6-deficient HIV or indirectly in the case of PTAP-deficient HIV. Our data also support the hypothesis that the main source of positive budding information in Gag lies not in p6 but instead in the MA-CA-NC region of the protein.

The most obvious support for these conclusions comes from the nearly normal budding of Gag(p47), the severe budding defect of Gag-SP2 (see Figure 1), and the robust budding of the NL4.3*(SP2$^{RPNF-KLSS}$/p6^{L1ter}) and NL4.3*(TF^{ter}/SP2^{I5ter}) viruses (see Figures 4 and 5). However, our conclusions are also supported by the more complex observations regarding PTAP-deficient HIVs. Specifically, we found that the p6$^{PTAP-LIRL}$ mutation caused an aberrant initial cleavage of Gag at the SP2/p6 junction, generating Gag(p49) through posttranslational proteolysis. This raised the possibility that the severe budding defect of PTAP-deficient HIV might also be mediated by activation of the IBS. In support of this hypothesis, we found that eliminating Gag-Pol (and therefore PR) expression allowed PTAP-deficient HIV to bud at nearly WT levels. Our

speculative model is also supported by the finding that IBS inactivation suppressed most of the budding defect of PTAP-deficient HIV, elevating it eightfold, to ~70% of WT control. Importantly, this new explanation for the budding defect of PTAP-deficient HIV resolves a long-recognized but previously inexplicable observation, that the budding defect of PTAP-deficient HIV requires the activity of the viral protease (Huang *et al.*, 1995).

Taken together, these data indicate that a new paradigm of PTAP function might lead to a better understanding of its role in HIV biology. On the basis of the data presented in this report, it seems as if the primary purpose of the PTAP motif is to regulate the PR-mediated cleavage of HIV Gag (and perhaps also Gag-Pol). Such a role is consistent with the fact that the production of infectious HIV requires a careful timing between PR-mediated cleavage of Gag and the budding of virions from the cell: If PR cleaves Gag too early, it will destroy the budding information in Gag and virions will not bud, but if PR cleaves too late, infectivity could also be reduced through incomplete maturation. The crucial question now is to understand how PTAP-TSG101 (and other p6–ESCRT interactions?) affects PR-mediated cleavage of Gag.

It should also be noted that many of our experiments demonstrated a slight positive role for the PTAP motif and the p6 domain in the budding of HIV and HIV Gag (up to 30% of total). Thus we are not suggesting that these elements play no role in budding or that p6–ESCRT interactions do not make a slight positive contribution to budding. However, we do conclude that such positive contributions to budding are relatively subtle and their loss makes only a minor contribution to the severe budding defects seen for p6-deficient and PTAP-deficient HIV.

The identification of the IBS provides new insights into some classic observations in the field of HIV budding, but it also highlights a previously unrecognized aspect of HIV biology: the role of the IBS. Two observations indicate that the IBS is a selected, positive component of the virus: first, its conservation among HIV strains and with SIV; and second, the fact that a single amino acid substitution in the IBS ($SP2^{P13L}$) reduced HIV infectivity to ~14% ($13.8 \pm 0.89\%$; $n = 5$) of control. These data indicate that IBS plays a positive role in the HIV life cycle, but what exactly is this role? Currently, we do not know. However, our data raise the possibility that the IBS exists to prevent the budding of Gag(p49). Intriguingly, our data indicate that the PTAP motif exists, in part, to prevent production of Gag(p49). Such complexity indicates that HIV goes to great lengths to prevent the formation and budding of Gag(p49). At first glance, this might seem an inordinately complex way to prevent virion incorporation of a protein that can be avoided simply eliminating the SP2/p6 cleavage site. However, it could be that these complex relationships between PR-mediated cleavage, budding, and ESCRT-binding sites might be the way that HIV achieves the proper coordination between virus budding and virus maturation. However, this is no more than a speculative model, and follow-up studies are required before we can attain a clear understanding of why HIV possess an IBS.

MATERIALS AND METHODS

Plasmids and antibodies

All amplified regions of all plasmids were sequenced, and only sequence-confirmed clones were used in the experiments. To make pcDNA3 plasmids designed to express HIV Gag(p49)-SF, EIAV Gag-SF, RSV Gag-SF, and HTLV-1 Gag-SF, we excised Asp-718–*Bam*HI fragments containing the corresponding Gag ORFs from pcDNA3-HIV Gag(p49)-GFP, pcDNA3-EIAV Gag-GFP, pcDNA3-RSV Gag-GFP, and pcDNA3-HTLV-1 Gag-GFP (Fang *et al.*, 2007) and inserted them between the Asp-718 and *Bam*HI sites of pcDNA3-SF, upstream of, and in frame with, the 61 codon–long SF tag ORF. The CD63 and CD81 ORFs were amplified using primers designed to append the same sites at their termini and also inserted upstream of and in frame with the SF tag of pcDNA3-SF to express CD63-SF and CD81-SF. The modified versions of these plasmids were amplified using oligonucleotides designed to append SP2* or a mutant form of SP2* to the C terminus of the encoded proteins. The VPS4B and VPS4B/K180Q ORFs were amplified using pDsRED-VPS4B and pDsRED-VPS4B/K180Q (generous gifts from W. Sundquist, University of Utah, Salt Lake City, UT) as template, using oligonucleotides that added an *Xho*I site upstream of the ORF and a *Not*I site downstream of the stop codon. The resulting fragments were cleaved with *Xho*I and *Not*I and inserted between the *Xho*I and *Not*I sites of pcDNA3-GFP (Booth *et al.*, 2006), downstream of and in frame with the GFP ORF, to create pcDNA3-GFP-VPS4B and pcDNA3-GFP-VPS4B/K180Q.

The plasmids designed to express HIV Gag (pcDNA3-HIV Gag) and Acyl-LZ-DsRED (pcDNA3-Acyl-LZ-DsRED) were described previously (Booth *et al.*, 2006; Fang *et al.*, 2007). All Gag mutants were based on pcDNA3-HIV Gag, amplified with an invariant 5′-end oligonucleotide and a 3′-end oligonucleotide that carried the desired mutation and a *Bam*HI site at its 5′ end. The amplification products were then cleaved with *Bsr*I and *Bam*HI and inserted between the *Bsr*I and *Bam*HI sites of pcDNA3-HIV Gag. The plasmid that expresses the mutant variant of Acyl-LZ-DsRED was generated by amplifying the ORF with oligonucleotides designed to append SP2* at the C terminus of the encoded protein and inserting it between the Asp-718 and *Bam*HI sites of pcDNA3.

Previous reports described the HIV proviruses pNL4-3-ΔE-GFP (Zhang *et al.*, 2004) and pNL4-3-ΔE-GFP/$p6^{L1ter}$ (Fang *et al.*, 2007). Mutations were introduced into these viruses by amplifying an ~800 base pairs–long internal *Apa*I-*Bsf*I fragment with primers that incorporated the desired mutation(s), cleaving the product with *Apa*I and *Sbf*I, and inserting the product between the *Apa*I and *Sbf*I sites of pNL4-3-ΔE-GFP/$p6^{L1ter}$ (Fang *et al.*, 2007). Again, all amplified regions of all plasmids were sequenced, and experiments were performed only with plasmids that had the desired DNA sequence.

Antibodies were obtained as follows: mouse anti-Gag monoclonal antibody (mAb) 3537 was from the AIDS reagent repository, mouse anti-Flag mAb F-3165 was from Sigma, rabbit anti-GFP A11122 was from Invitrogen, control rabbit immunoglobulin (Ig) G was from Sigma, anti–β-tubulin antibody 556321 was from BD PharMingen, and secondary antibodies conjugated to horseradish peroxidase (HRP) or fluorophores were from Jackson ImmunoResearch (West Grove, PA).

Cell culture, transfection, and microscopy

293T cells were maintained in DMEM supplemented with 10% fetal bovine serum and transfected by electroporation (Chang *et al.*, 1997) (for immunoblot and IP experiments) using a BTX ECM 600 electroporator, or by lipofection (for immunofluorescence and electron microscopy) using Lipofectamine 2000 (Invitrogen, Carlsbad, CA). 293T cells were processed for immunofluorescence microscopy (Booth *et al.*, 2006) using rabbit polyclonal antibodies specific for HIV Gag, mouse monoclonal antibodies specific for the Flag tag, and fluorescein isothiocyanate– or Texas Red–labeled secondary antibodies. Immunofluorescence images were obtained at room temperature on a BH2-RFCA microscope (Olympus, Center Valley, PA) equipped with an Olympus S-Plan-Apo 60× 0.40 oil objective and a Sensicam QE (Cooke, Romulus, MI) digital camera using IPLab 3.6.3 software (Scanalytics, Reutlingen, Germany). Images were converted

to TIFF files, imported into Photoshop CS, and assembled into figures using Illustrator CS (Adobe Systems, San Jose, CA). For transmission electron microscopy, 293T cells were fixed, processed, and examined as described previously for Jurkat T-cells (Booth *et al.*, 2006; Fang *et al.*, 2007).

EMV/virus preparations, immunoblot, coimmunoprecipitation, density gradient analysis, and gel filtration

EMVs and viruses were collected from the medium as described previously (Booth *et al.*, 2006; Fang *et al.*, 2007). For immunoblot experiments, cells were transfected and incubated for 2 d, EMVs/viruses were collected (Booth *et al.*, 2006; Fang *et al.*, 2007), and cells and EMVs/viruses were lysed in SDS–PAGE sample buffer. Each sample was separated by SDS–PAGE, transferred to PVDF membranes, and processed for immunoblot using specific primary antibodies and HRP-conjugated secondary antibodies, followed by chemiluminescent detection and detection of proteins by exposure of x-ray film. Films were scanned and converted to TIFF files, and the signal for each band was quantified using ImageJ software. Budding efficiencies were calculated from extent of budding (vesicle/vesicle + cell), relative to that of the positive control. For those experiments that were performed three or more times, the data are also presented as the average ± 1 SD, along with the p value from a Student's *t* test.

For co-IP experiments, 293T cells were transfected with plasmids encoding both test proteins, at a 1:1 ratio, and incubated for 2 d. Cells were then resuspended in RIPA buffer (50 mM Tris-HCl, pH 7.4, 150 mM NaCl, 1% NP-40, 1 mM EDTA, and a protease inhibitor cocktail; Roche, Basel, Switzerland) at 4°C, lysed by freeze–thaw (two cycles), and clarified by centrifugation at 16,000 × *g* for 10 min. The resulting supernatant was precleared by incubating with protein A beads (Sigma) and nonimmune rabbit IgG for 2 h at 4°C. The beads were removed, each sample was split in half, one-half was incubated O/N at 4°C with nonimmune rabbit IgG, and the other half was incubated O/N at 4°C with rabbit polyclonal antibodies to GFP. Each sample was incubated with protein A beads for 2 h at 4°C, and the beads were washed six times with RIPA buffer and boiled in SDS–PAGE loading buffer. Samples were then separated by SDS–PAGE, transferred to PVDF membranes, and processed for immunoblot using mouse monoclonal antibodies specific for either the flag tag or HIV Gag.

For density gradient centrifugation experiments, we transfected 293T cells with plasmids designed to express Gag or Gag-SP2, incubated the cells for 2 d, washed the cells in cold phosphate-buffered saline (PBS) (4°C), scraped from the tissue culture dish, and pelleted by centrifugation at 600 × *g* for 5 min. Cell pellets were washed once with 10 mM Tris-HCl (pH 7.4) containing 1 mM ethylene glycol tetraacetic acid and once with 10 mM Tris-HCl (pH 7.4) containing 1 mM EDTA and then resuspended in TE buffer (10 mM Tris-HCl containing 1 mM EDTA), 10% (wt/vol) sucrose, and Complete Protease Inhibitor Cocktail (Roche). Cells were then lysed by sonication. Lysates were pelleted by spinning at 2000 rpm for 3 min in an Eppendorf Microfuge to remove unbroken cells and nuclei. Each sample was resuspended in TE buffer, and 0.25 ml of each was added to 1.5-ml microcentrifuge tubes. One was untreated, one was adjusted to 0.25% Triton X-100 and incubated at 37°C for 20 min, and one was adjusted to 0.25% Triton X-100 and incubated at 4°C for 20 min. Then 1.25 ml cold 85.5% (wt/vol) sucrose/TE buffer was added to each of the three tubes, and these were placed on the bottom of a centrifuge tube. To each we layered 7 ml 65% (wt/vol) sucrose/TE and then 3.25 ml 10% (wt/vol) sucrose/TE. The gradients were then spun at 100,000 × *g* for 18 h at 4°C in a Beckman SW41 rotor. At the conclusion of the spin, we collected 10 1.2-ml fractions from the top of the centrifuge tube and processed each for immunoblot using antibodies specific for Gag.

For gel filtration experiments, we transfected 293T cells with plasmids designed to express Gag or Gag-SP2, incubated the cells for 2 d, washed the cells in cold PBS (4°C), lysed the cells in RIPA buffer (50 mM Tris, pH 7.4, 150 mM NaCl, 1 mM EDTA, 1% NP-40, protease inhibitor cocktail [Roche]) by two freeze–thaw cycles, and clarified the lysates by passing them through a 0.22-µm filter. Before fractionation of the clarified lysates, we generated a pair of Sephacryl-500 HR resin (GE Healthcare, Piscataway, NJ) columns (1 cm diameter) by loading two columns each with a slurry of 15 ml Sephacryl-500 HR resin and 4 ml gel filtration buffer (50 mM Tris, pH 7.4, 150 mM NaCl, 1 mM EDTA). Columns were packed by flowing gel filtration buffer through the resin for 2 h at 1 ml/min and then for 1 h at 2.3 ml/min. Then 0.5 ml of each lysate was loaded at the top of the column and fractionated by flowing gel filtration buffer at 1.5 ml/min. Fifteen 1-ml fractions were collected from each column, and each fraction was examined by immunoblot using antibodies specific for HIV Gag and β-tubulin.

HIV infectivity measurements

To determine the relative infectivity of different HIV proviruses, we adapted an established assay (Zhang *et al.*, 2004) as follows. First, 6.7 µg of each HIV provirus plasmid was cotransfected with 3.3 µg of pVSV-G into 7.5×10^6 293T cells by electroporation. Two days later the tissue culture supernatants were collected, and the cells were fixed and examined by fluorescence microscopy to determine the percentage of cells expressing the provirus-encoded GFP protein (NL4.3* encodes a modified form of GFP that is localized to the lumen of the endoplasmic reticulum [Zhang *et al.*, 2004]). The tissue culture supernatants were processed by passage through a 0.2-µm filter and pelleted by centrifugation at 70,000 × *g* for 1 h. Each pellet was resuspended in 30 µl RPMI medium supplemented with 20% fetal calf serum (FCS), and 1 µl of each was mixed with 5×10^5 $CD4^+$ T-cells (Jurkat). The cell/virus mixtures were then spun at 1200 × *g* for 2 h at room temperature. Each cell/virus mixture was then resuspended in 1 ml RPMI supplemented with 20% FCS and incubated for an additional 2 d. The cells were then fixed and examined by fluorescence microscopy to determine the number of cells expressing the virus-encoded GFP. These experiments included an initial titration of control virus preparations to ensure the percentage of Jurkat cells infected by the WT control provirus was ~15%, within the linear range of the assay (Zhang *et al.*, 2004). Each experiment was performed a minimum of three times, and the data are presented as the average ± 1 SD, along with the p value from a Student's *t* test.

ACKNOWLEDGMENTS

We thank L. Shen and R. Siliciano for teaching us how to perform the HIV infectivity assay and Jef Boeke, Michael Caterina, and Dan Raben for constructive comments during the course of the study. This work was supported by the National Institutes of Health (DK-45787) and the Johns Hopkins Fund for Medical Discovery.

REFERENCES

Alais S, Simoes S, Baas D, Lehmann S, Raposo G, Darlix JL, Leblanc P (2008). Mouse neuroblastoma cells release prion infectivity associated with exosomal vesicles. Biol Cell 100, 603–615.

Benit L, De Parseval N, Casella JF, Callebaut I, Cordonnier A, Heidmann T (1997). Cloning of a new murine endogenous retrovirus, MuERV-L, with strong similarity to the human HERV-L element and with a gag coding sequence closely related to the Fv1 restriction gene. J Virol 71, 5652–5657.
Bieniasz PD (2009). The cell biology of HIV-1 virion genesis. Cell Host & Microbe 5, 550–558.
Booth AM, Fang Y, Fallon JK, Yang JM, Hildreth JE, Gould SJ (2006). Exosomes and HIV Gag bud from endosome-like domains of the T cell plasma membrane. J Cell Biol 172, 923–935.
Chang CC, Lee WH, Moser H, Valle D, Gould SJ (1997). Isolation of the human PEX12 gene, mutated in group 3 of the peroxisome biogenesis disorders. Nat Genet 15, 385–388.
Cocucci E, Racchetti G, Meldolesi J (2009). Shedding microvesicles: artefacts no more. Trends Cell Biol 19, 43–51.
Demirov DG, Orenstein JM, Freed EO (2002). The late domain of human immunodeficiency virus type 1 p6 promotes virus release in a cell type-dependent manner. J Virol 76, 105–117.
Dukers DF, Meij P, Vervoort MB, Vos W, Scheper RJ, Meijer CJ, Bloemena E, Middeldorp JM (2000). Direct immunosuppressive effects of EBV-encoded latent membrane protein 1. J Immunol 165, 663–670.
Edidin M (2003). The state of lipid rafts: from model membranes to cells. Annu Rev Biophys Biomol Struct 32, 257–283.
Fang Y, Wu N, Gan X, Yan W, Morrell JC, Gould SJ (2007). Higher-order oligomerization targets plasma membrane proteins and HIV gag to exosomes. PLoS Biol 5, 1267–1283.
Fevrier B, Vilette D, Archer F, Loew D, Faigle W, Vidal M, Laude H, Raposo G (2004). Cells release prions in association with exosomes. Proc Natl Acad Sci USA 101, 9683–9688.
Freed EO (1998). HIV-1 gag proteins: diverse functions in the virus life cycle. Virology 251, 1–15.
Freed EO, Martin MO (2006). HIVs and their replication. In: Fields Virology, vol. 2, ed. DM Knipe, PM Howley, Philadelphia: Lippincott Williams & Wilkins, 2107–2185.
Garrus *et al*. JE (2001). Tsg101 and the vacuolar protein sorting pathway are essential for HIV-1 budding. Cell 107, 55–65.
Gottlinger HG, Dorfman T, Sodroski JG, Haseltine WA (1991). Effect of mutations affecting the p6 gag protein on human immunodeficiency virus particle release. Proc Natl Acad Sci USA 88, 3195–3199.
Gould SJ, Booth AM, Hildreth JE (2003). The Trojan exosome hypothesis. Proc Natl Acad Sci USA 100, 10592–10597.
Hanson PI, Shim S, Merrill SA (2009). Cell biology of the ESCRT machinery. Curr Opin Cell Biol 21, 568–574.
Hsu C *et al*. (2010). Regulation of exosome secretion by Rab35 and its GTPase-activating proteins TBC1D10A-C. J Cell Biol 189, 223–232.
Huang M, Orenstein JM, Martin MA, Freed EO (1995). p6Gag is required for particle production from full-length human immunodeficiency virus type 1 molecular clones expressing protease. J Virol 69, 6810–6818.
Hurley JH (2008). ESCRT complexes and the biogenesis of multivesicular bodies. Curr Opin Cell Biol 20, 4–11.
Keller S, Konig AK, Marme F, Runz S, Wolterink S, Koensgen D, Mustea A, Sehouli J, Altevogt P (2009). Systemic presence and tumor-growth promoting effect of ovarian carcinoma released exosomes. Cancer Lett 278, 73–81.
Kolotuev I, Apaydin A, Labouesse M (2009). Secretion of Hedgehog-related peptides and WNT during *Caenorhabditis elegans* development. Traffic (Copenhagen, Denmark) 10, 803–810.
Krishnamoorthy L, Bess JW Jr, Preston AB, Nagashima K, Mahal LK (2009). HIV-1 and microvesicles from T cells share a common glycome, arguing for a common origin. Nat Chem Biol 5, 244–250.
Leblanc P, Alais S, Porto-Carreiro I, Lehmann S, Grassi J, Raposo G, Darlix JL (2006). Retrovirus infection strongly enhances scrapie infectivity release in cell culture. EMBO J 25, 2674–2685.
Liegeois S, Benedetto A, Garnier JM, Schwab Y, Labouesse M (2006). The V0-ATPase mediates apical secretion of exosomes containing Hedgehog-related proteins in *Caenorhabditis elegans*. J Cell Biol 173, 949–961.
Lingwood D, Kaiser HJ, Levental I, Simons K (2009). Lipid rafts as functional heterogeneity in cell membranes. Biochem Soc Trans 37, 955–960.
Logozzi M *et al*. (2009). High levels of exosomes expressing CD63 and caveolin-1 in plasma of melanoma patients. PloS One 4, e5219.
Loomis RJ, Holmes DA, Elms A, Solski PA, Der CJ, Su L (2006). Citron kinase, a RhoA effector, enhances HIV-1 virion production by modulating exocytosis. Traffic (Copenhagen, Denmark) 7, 1643–1653.
Marsh M, Theusner K, Pelchen-Matthews A (2009). HIV assembly and budding in macrophages. Biochem Soc Trans 37, 185–189.
Morita E, Sundquist WI (2004). Retrovirus budding. Annu Rev Cell Dev Biol 20, 395–425.
Nazarenko I, Rana S, Baumann A, McAlear J, Hellwig A, Trendelenburg M, Lochnit G, Preissner KT, Zoller M (2010). Cell surface tetraspanin Tspan8 contributes to molecular pathways of exosome-induced endothelial cell activation. Cancer Res 70, 1668–1678.
Nguyen DH, Hildreth JE (2000). Evidence for budding of human immunodeficiency virus type 1 selectively from glycolipid-enriched membrane lipid rafts. J Virol 74, 3264–3272.
Ono A, Freed EO (2001). Plasma membrane rafts play a critical role in HIV-1 assembly and release. Proc Natl Acad Sci USA 98, 13925–13930.
Ostrowski M *et al*. (2010). Rab27a and Rab27b control different steps of the exosome secretion pathway. Nat Cell Biol 12, 19–30.
Pan BT, Johnstone RM (1983). Fate of the transferrin receptor during maturation of sheep reticulocytes in vitro: selective externalization of the receptor. Cell 33, 967–978.
Paxton W, Connor RI, Landau NR (1993). Incorporation of Vpr into human immunodeficiency virus type 1 virions: requirement for the p6 region of gag and mutational analysis. J Virol 67, 7229–7237.
Saksena S, Sun J, Chu T, Emr SD (2007). ESCRTing proteins in the endocytic pathway. Trends Biochem Sci 32, 561–573.
Savina A, Vidal M, Colombo MI (2002). The exosome pathway in K562 cells is regulated by Rab11. J Cell Sci 115, 2505–2515.
Schorey JS, Bhatnagar S (2008). Exosome function: from tumor immunology to pathogen biology. Traffic (Copenhagen, Denmark) 9, 871–881.
Simons M, Raposo G (2009). Exosomes—vesicular carriers for intercellular communication. Curr Opin Cell Biol 21, 575–581.
Skog J, Wurdinger T, van Rijn S, Meijer DH, Gainche L, Sena-Esteves M, Curry WT Jr, Carter BS, Krichevsky AM, Breakefield XO (2008). Glioblastoma microvesicles transport RNA and proteins that promote tumour growth and provide diagnostic biomarkers. Nat Cell Biol 10, 1470–1476.
Strack B, Calistri A, Craig S, Popova E, Gottlinger HG (2003). AIP1/ALIX is a binding partner for HIV-1 p6 and EIAV p9 functioning in virus budding. Cell 114, 689–699.
Thery C, Ostrowski M, Segura E (2009). Membrane vesicles as conveyors of immune responses. Nat Rev Immunol 9, 581–593.
Thery C, Zitvogel L, Amigorena S (2002). Exosomes: composition, biogenesis and function. Nat Rev Immunol 2, 569–579.
Trajkovic K, Hsu C, Chiantia S, Rajendran L, Wenzel D, Wieland F, Schwille P, Brugger B, Simons M (2008). Ceramide triggers budding of exosome vesicles into multivesicular endosomes. Science 319, 1244–1247.
Trams EG, Lauter CJ, Salem N Jr, Heine U (1981). Exfoliation of membrane ecto-enzymes in the form of micro-vesicles. Biochim Biophys Acta 645, 63–70.
Valadi H, Ekstrom K, Bossios A, Sjostrand M, Lee JJ, Lotvall JO (2007). Exosome-mediated transfer of mRNAs and microRNAs is a novel mechanism of genetic exchange between cells. Nat Cell Biol 9, 654–659.
Wollert T, Wunder C, Lippincott-Schwartz J, Hurley JH (2009). Membrane scission by the ESCRT-III complex. Nature 458, 172–177.
Yu X, Harris SL, Levine AJ (2006). The regulation of exosome secretion: a novel function of the p53 protein. Cancer Res 66, 4795–4801.
Yu X, Riley T, Levine AJ (2009). The regulation of the endosomal compartment by p53 the tumor suppressor gene. FEBS J 276, 2201–2212.
Zhang H *et al*. (2004). Novel single-cell-level phenotypic assay for residual drug susceptibility and reduced replication capacity of drug-resistant human immunodeficiency virus type 1. J Virol 78, 1718–1729.